Abdel-Malek, K., Blackmore, D., and Joy, K., (submitted), "Swept Volumes: Foundations, Perspectives, and Applications", *International Journal of Shape Modeling.*

Swept Volumes: Foundations, Perspectives, and Applications

Karim Abdel-Malek
Department of Mechanical Engineering and Center for Computer Aided Design
University of Iowa
Iowa City, IA 52242
Tel: 319-335-5676
Amalek@engineering.uiowa.edu

Denis Blackmore
Department of Mathematical Sciences
New Jersey Institute of Technology
Newark, New Jersey 07102
Tel: 201-596-3495
Deblac@chaos.njit.edu

Kenneth Joy
Computer Science Department
University of California Davis
Davis, California 95616
Tel: 1-530-752-1077
Joy@cs.ucdavis.edu

Abstract

Several fundamental developments in the past decade have led to a better understanding of swept volumes. While the underlying formulation for characterizing the volume generated as a result of the motion of a geometric entity in space has appeared in various fields under different names, this review seeks to unify the terminology and demonstrate the applicability to different fields. This paper reviews the various formulations that have appeared, outlines the basic research involved, and highlights the implications on research in engineering, mathematics, and computer science. The applicability of this seemingly simple formulation to the fields of solid modeling, robotics, manufacturing automation, and visualization is demonstrated through results reported by the authors, each in their own field.

Keywords: Swept volumes, workspace analysis, NC verification, solid modeling.

1.0 Historical Remarks

Attempts were made to obtain the exact swept volume of the motion of a rigid body in space in the early 1960's using a combination of calculus and graphical techniques. . We define a swept volume as the volume generated by the motion of an arbitrary object along an arbitrary path (or even a surface) possibly with arbitrary rotations. The problem of swept volume determination is concerned with the calculation of properties associated with the resulting sweep, including the delineation of the boundary for visualization and computer graphics, formulations for modeling the sweep procedure, and the calculation of the volume's mass properties for solid modeling. Perhaps the most challenging problem facing this field has been the identification and visualization of the boundary, especially for those volumes that are based on freeform geometric entities. The concept of determining the so-called necessary boundary at several steps during the sweep have been used in early works (although still used today in some implementations), where

intermediate frames are computed, their necessary boundary identified, and finally all boundaries are connected (see Fig. 1).

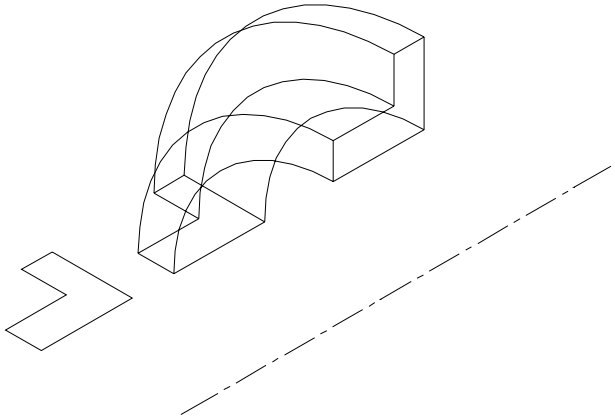

Fig. 1 Sweeping of a geometric entity

While the mathematics used in treating sweep problems have become more sophisticated, the idea remains the same. The goal is to determine, mathematically or not, the outer boundary of the object (also called the generator) during its motion from an initial to a final position and orientation. The main difficulty has been (and remains to some extent) the identification of this boundary, obtaining an accurate representation, and the development of fundamental formulations implementable in computer code.

Although some researchers have investigated what seemed to be efficient methods, they were faced with problems of visualization because of the limited computational power available at that time. In fact, the field of descriptive geometry has addressed similar issues (Wellman 1957). Until recently, the problem of computing the swept volume was thought to be hindered by seemingly complex mathematics and the self-intersection of the generated volume. Many researchers presented solutions varying from implicit approaches (Klok 1986) to the numerical implicit solutions (Schroeder, et al. 1994 and Ganter, et al. 1993).

Indeed, many have addressed specific problems pertaining to swept volumes. For example, Kim and Moon (1990) presented an algebraic algorithm for generating the purely rotational sweeping volumes of planar objects bounded by algebraic curves. The sweep volume boundary is related to convolutions consisting of the planar object boundaries at its start and final angles and the circular sweep arcs of radial extreme points. Parida and Mudur (1994) identified a sufficiently general class of swept objects and have classified the sweep rules. Although some believe that swept volume methods employ the similar mathematics to that of offsets and Minkowski Sums (Elber and Kim 1999, Maekawa 1999, and Ahn, *et al.* 1997), we believe that formalisms for addressing swept volumes are very different that those for offsets. A different approach using a surface fitting algorithm for sweep surface reconstruction from three-dimensional measured data was presented by Ueng, et al. (1998), but limited to translational sweeping in which the generators traverse about the directors to form the desired sweep surface.

A formulation for developing a geometric representation of swept volumes for compact *n*-manifolds undergoing general sweeps in $\mathbf{R}^n$ was presented by Weld and Leu (1990) as an extension of the work by Wang and Wang (1986). It was shown that the swept volume of a compact *n*-manifold in $\mathbf{R}^n$ is equal to the

union of the swept volume of its boundary with one location of the compact *n*-manifold in the sweep. Based on this formulation, the swept volumes of polyhedral objects were generated from the swept volumes of their polygonal faces. The work by Wang and Wang was continued by a colleague of the first author and in collaboration with a mathematician at NJIT (second author of this paper).

In 1990, Blackmore and Leu introduced a new type of formulation, whereby every smooth Euclidean motion, or sweep, can be identified with a first-order, linear, ordinary differential equation. The so-called Sweep Differential Equation (SDE) method provided useful insights into the topological and geometrical nature of the swept volume of an object and will be further explored below.

Singularity theory (also referred to as Manifold stratification or Jacobian rank deficiency method [Abdel-Malek and Yeh 1997a and Abdel-Malek and Othman 1999]) was shown to address the determination of the boundary volume obtained as a result of multiple sweeping (multiple sweeping is a term that denotes the generation of a volume in space whereby an entity is arbitrarily swept several times adding a number of sweep parameters to the sweep equation). It was shown that by an appropriate manipulation of the sweep Jacobian, it is possible to stratify the Jacobian to obtain *exact* boundary surface patches in closed form (also called strata). The method was expanded in recent years and was shown to address outstanding problems in robotics, manufacturing automation, and ergonomics.

In the following section, we will first introduce the fundamental concepts associated with sweeping using a simple examples, will introduce the formulation therein, and will explore both specialized and common problems associated with sweeping, implementation, and applications.

2.0 Modeling

The fundamental theory of swept volumes is rooted in the Implicit Function Theorem. We first illustrate a simple example to motivate the discussion. We will then address two formulations that have recently appeared that treat the problem of swept volumes using (1) Manifold Stratification and (2) Sweep Envelope Differential Equation (SEDE) method.

2.1 Simple Example:

Consider a given curve specified by the parabola

$$y = 4 - x^2 \;\; ; \;\; -2 \le x \le 1 \tag{1}$$

shown in Fig. 2, or in parametric form as

$$\mathbf{\Gamma}(s) = [s \quad 4 - s^2]^T; \; -2 \le s \le 1 \tag{2}$$

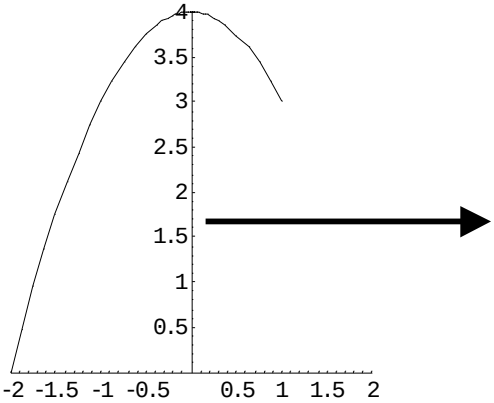

Fig. 2 A parabola defined on an interval $-2 \le x \le 1$

This curve is to be swept in the *x*-direction along the path given by

$$[t \quad 0]^T;\ 0 \le t \le 5 \tag{3}$$

The sweep equation is defined as

$$\xi(s,t) = [s+t \quad 4-s^2]^T;\ -2 \le s \le 1 \text{ and } 0 \le t \le 5 \tag{4}$$

This equation represents a sweep in the *xy*-plane.

In order to define the boundary of this sweep, we substitute the limits for each parameter. For example, substituting the limit $s = -2$ into $\xi(s,t)$ yields the equation of a line denoted by ℓ_1 defined by $[t-2 \quad 0]^T$ on the interval $t \in [0,\ 5]$. Substituting the limit $s = 1$ yields the line ℓ_2 defined as $[t+1 \quad 3]^T$ on the same interval. Similarly, substituting the limit for $t = 0$ yields the equation of the original curve denoted by ℓ_3 and defined by $[s \quad 4-s^2]^T$. Substituting $t = 5$ yields the parabola after it has translated along the *x*-axis by five units as ℓ_4 defined by $[s+5 \quad 4-s^2]^T$ also on the interval $s \in [-2,\ 1]$. The plots of $\ell_1 - \ell_4$ are shown in Fig. 3.

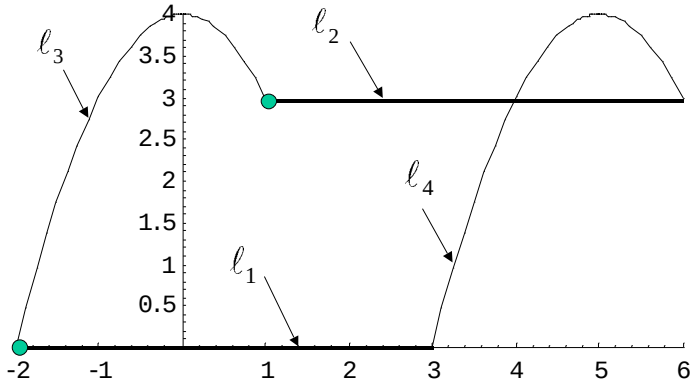

Fig. 3 Determination of curves

Two remarks:

(1) Some curves that must be on the boundary are still missing (in particular, the line segment joining the tip of each curve).

(2) The curves that have been determined thus far may or may not be on the boundary.

To determine the missing curve, one must find the global/local maximum point on the curve in the direction of sweep (i.e, the tip of the parabola). In this case, the local and global maximum for the parabola is at $s = 0$ obtained by differentiating the curve with respect to *s* and setting the result to zero. Substituting $s = 0$ into the sweep equation yields the curve denoted by ℓ_5 and shown in Fig. 4.

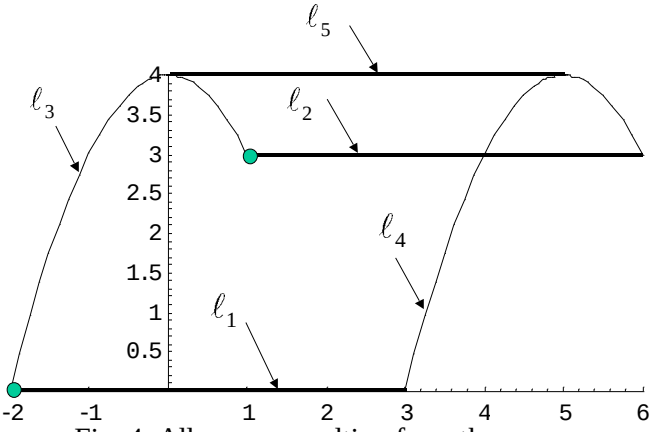

Fig. 4 All curves resulting from the sweep

Once all curves are determined, it is now necessary to identify those curves that are on the boundary by eliminating all curve segments inside the swept region. This problem has been denoted by various designations such as trimming (Blackmore, *et al.* 1999), boundary identification (Abdel-Malek and Yeh 1997a), and clipping (Madrigal and Joy 1999). For this example, removal of internal curves (those that are

not on the boundary) is performed and the result is indeed the swept region shown in Fig. 5 (note that the term swept volume is typically used even if the region is two-dimensional).

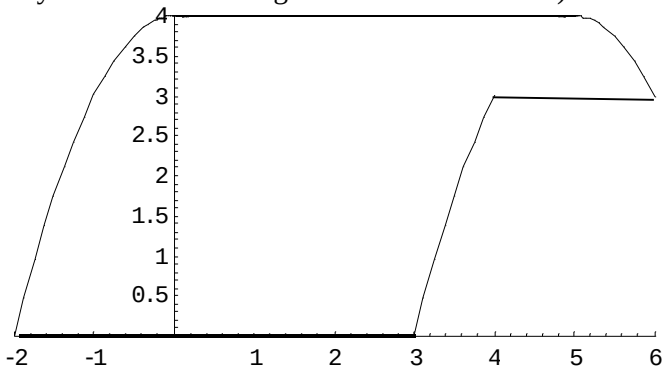

Fig. 5 The resulting swept region

Note that if the curve above is swept along the *y*-axis instead, only its endpoints would yield curves and a maximum cannot be found. This simple idea can be extended into a generalized formulation by investigating the Taylor Series expansion of a vector function of several variables denoted by $\boldsymbol{\xi}(\mathbf{q})$, where $\mathbf{q} = [q_1 \quad \ldots \quad q_n]^T$, where q_i are the sweep parameters (i.e., $\mathbf{q} = \begin{bmatrix} s & t \end{bmatrix}^T$) in the previous example.

$$\boldsymbol{\xi}(\mathbf{q}) = \boldsymbol{\xi}(\mathbf{q}^o) + \nabla\boldsymbol{\xi}(\mathbf{q}^o)^T(\mathbf{q}-\mathbf{q}^o) + 0.5(\mathbf{q}-\mathbf{q}^o)\mathbf{H}(\mathbf{q}^o)(\mathbf{q}-\mathbf{q}^o) + R \tag{5}$$

where **H** is the Hessian of $\boldsymbol{\xi}$ and *R* represents higher order terms. A change in the function represented by its gradient is given as

$$\nabla\boldsymbol{\xi} = \nabla\boldsymbol{\xi}(\mathbf{q}^o)^T(\mathbf{q}-\mathbf{q}^o) + 0.5(\mathbf{q}-\mathbf{q}^o)\mathbf{H}(\mathbf{q}^o)(\mathbf{q}-\mathbf{q}^o) + R \tag{6}$$

If we assume a local minimum then $\nabla\boldsymbol{\xi}$ must be nonnegative, i.e., $\nabla\boldsymbol{\xi} \geq 0$. Concentrating only the first-order term in Eq. (6), we observe (as before) that $\nabla\boldsymbol{\xi}$ can be nonnegative for all possible $(\mathbf{q}-\mathbf{q}^o)$ when

$$\nabla\boldsymbol{\xi}(\mathbf{q}^o) = \mathbf{0} \tag{7}$$

In the case of a vector function $\boldsymbol{\xi}(\mathbf{q})$, the equivalent of Eq. (b) is

$$\nabla\boldsymbol{\xi} = \mathbf{J}(\mathbf{q}^o)^T(\mathbf{q}-\mathbf{q}^o) + R \tag{8}$$

where $\mathbf{J} = \left[\partial\boldsymbol{\xi}/\partial\mathbf{q}\right] = \boldsymbol{\xi}_{\mathbf{q}}$ and setting the gradient of a function of several variables to zero is equivalent to setting the determinant of its square Jacobian matrix $\mathbf{J}$ to zero (i.e., finding a singular point). Therefore, for a 3D vector ($\boldsymbol{\xi}$) with three variables, the Jacobian is a (3×3) matrix, whose determinant is an analytic function. The complexity in analysis arises when many variables are used to define the sweep (i.e., more than three variables), resulting in a non-square Jacobian.

In order to have a well-posed formulation, constraints that are used to model the geometry of this problem should be independent, except at certain critical surfaces in the manifold (**Implicit Function Theorem**) where the Jacobian becomes singular. However, for sweeps with more than 3 parameters, the sweep Jacobian is not square. It is important, therefore, that there not be open sets in the space of the generalized parameters in which the constraints are redundant.

2.2 Sweep Equations

Consider a surface parameterized in terms of two variables as a (3×1) vector given by $\boldsymbol{\Gamma}(\mathbf{u})$, where $\mathbf{u} = \begin{bmatrix} u_1 & u_2 \end{bmatrix}^T$. This surface will be swept along a specified path given by the (3×1) vector $\boldsymbol{\Psi}(v)$, where the orientation of the surface is defined by a (3×3) rotation matrix denoted by $\mathbf{R}(v)$. The sweep equation generated by the motion of $\boldsymbol{\Gamma}(\mathbf{u})$ on $\boldsymbol{\Psi}(v)$ is defined as

$$\boldsymbol{\xi}(u_1, u_2, v) = \mathbf{R}(v)\boldsymbol{\Gamma}(u_1, u_2) + \boldsymbol{\Psi}(v) \tag{9}$$

where $\boldsymbol{\xi}$ characterizes the set of all points inside and on the boundary of the swept volume.

To define stationary points (in this case it may be sets of constant parameters or sets of parameters defined as a function of other variables), consider the derivative of the accessible set (Eq. 9) with respect to time as

$$\dot{\boldsymbol{\xi}}(\mathbf{q}) = \left[\frac{\partial \xi_i(\mathbf{q})}{\partial q_j}\right]\dot{\mathbf{q}} \tag{10}$$

where the dot denotes a derivative with respect to time and the matrix

$$\mathbf{J}(\mathbf{q}) = \left[\frac{\partial \xi_i(\mathbf{q})}{\partial q_j}\right] \tag{11}$$

is called the Jacobian of the sweep (or sweep Jacobian) and has dimension 3×3. The left-hand side of Eq. (10) is the velocity $\begin{bmatrix}\dot{x} & \dot{y} & \dot{z}\end{bmatrix}^T$ of a point moving in the swept volume having a parameter velocity vector $\dot{\mathbf{q}}$. The physical significance of the Jacobian was thoroughly explained and used in the study of the motion of robot manipulators (Abdel-Malek, *et al.* 1999a). In order to determine stationary points, the Jacobian is studied for rank deficiency. Because the Jacobian is square, its determinant is equated to zero and solved for constant values (or expressions) that make the Jacobian singular. The term **singularity** (singular set) is given to those values or expressions.

This Jacobian determinant singularity has been the fundamental underlying theory of the so-called sweep **envelope theory**, which has been consistently limited to 3 parameter sweep until recent work by Abdel-Malek and Yeh (1997a) and Abdel-Malek and Othman (1999). Early use of envelope theory is attributed to Dahlberg and Johansson (1987), Flaquer, et al. (1992), and Ganter and Uicker (1986) where it was used by the latter for detecting collisions and Wang and Wang (1986) where it was demonstrated for simulating the NC machining process (see the theory by Boltianskii 1964). Envelope theory was used by Martin and Stephenson (1989; 1990) to depict the swept volume of simple solids and by Hu and Ling (1994; 1995; 1996) to generate characteristic curves that are the point sets on the boundary of the generator at different times. The characteristic curves of the natural quadric surfaces (planes, circular cylinders, circular cones and spheres) were derived from the envelope theorem, which is also termed the instantaneous screw axis theorem in the field of kinematics, and it was used to describe the sweep motion of the generators. The faceted model of a swept volume is then established by warping the corresponding characteristic curves together with the partial boundaries of the generator at the initial and final positions.

Numerical methods to generate swept surfaces and volumes using implicit modeling techniques were also reported (Schroeder, et al. 1994). The algorithm reportedly treats degenerate trajectories such as self-intersections and surface singularity. Applications of this algorithm to maintainability design and robot path planning were demonstrated. More recently, still, an expansion of the Jacobian (3×3) singularity, Madrigal and Joy (1999) swept a Bezier surface to generate a solid of three variables (called a Trivariate Bezier Solid) and showed that characteristic curves can be computed even for the complex Bezier surfaces (this work will be explored in more detail in the Solid Modeling section). Recent works that have demonstrated methods for computing swept volumes are (Ling and Chase 1996 and Sourin and Pasko 1996). Other works that are related to swept volume formulations include ray representation methods (Hartquist, et al. 1999), methods for handling specific types of sweeping (Jüttler and Wagner 1999), and methods for improving the approximation of swept volumes (Elber 1997).

To summarize, all of the above methods for formulating the sweep equation or the sweep differential equation have been able to address very important problems, pertaining to boundary identification, visualization, and mathematical representation. However, these methods although they have the potential for expansion to multiple parameters, have been limited to three parameters.

2.3 Multi-parameter Sweeps (e.g., multivariate solids)

Using the formalism of shape feature languages, Jakubowski (1993) developed a multiple sweeping method for product modeling. A geometric entity with more than two parameters (a surface, a volume, or a *n*-dimensional entity) parametrized in terms of one or more variables as a (3×1) vector given by $\mathbf{\Gamma}(\mathbf{u})$, where $\mathbf{u}=[u_1 \quad \ldots \quad u_n]^T$, that is swept in space has also been considered (Abdel-Malek and Othman 1999) using the a systematic method for consecutive sweep representation adopted from kinematics (Denavit and Hartenberg 1955). Multiple arbitrary sweeps are performed to generate a complex solid, the result of which has been called a *multivariate solid* (Abdel-Malek and Yang 2000). Let the path also be defined by $\mathbf{\Psi}_1(v_1)$ and the orientation defined by $\mathbf{R}_1(v_1)$ such that the sweep equation is

$$\mathbf{N}_1(\mathbf{q})=\left[x(\mathbf{q}) \quad y(\mathbf{q}) \quad z(\mathbf{q})\right]^T=\mathbf{R}_1(v_1)\mathbf{\Gamma}(\mathbf{u})+\mathbf{\Psi}_1(v_1) \tag{12}$$

where $\mathbf{q}$ is the vector of *generalized coordinates* defined by $\mathbf{q}=[q_1 \quad \ldots \quad q_n]^T=\left[u_1 \quad \ldots \quad u_n \quad v_1\right]^T$ and $\mathbf{R}_1(v_1)$ is the (3×3) rotation matrix defining the orientation of the swept entity. In fact, $\mathbf{N}_1(\mathbf{q})$ characterizes the set of all points that belong to the volume. Another sweep motion with an orientation $\mathbf{R}_2(v_2)$ and along the path $\mathbf{\Psi}_2$ yields an expanded swept volume in the form of

$$\mathbf{N}_2(\mathbf{q})=\mathbf{R}_2(v_2)\mathbf{N}_1(\mathbf{q})+\mathbf{\Psi}_2(v_2)=\mathbf{R}_2\mathbf{R}_1\mathbf{\Gamma}+\mathbf{R}_2\mathbf{\Psi}_1+\mathbf{\Psi}_2 \tag{13}$$

where now $\mathbf{q}=[u_1 \quad \ldots \quad u_n \quad v_1 \quad v_2]^T$. Consecutive sweeps yield a modified set defined by

$$\mathbf{N}_3=\mathbf{R}_3\mathbf{R}_2\mathbf{R}_1\mathbf{\Gamma}+\mathbf{R}_3\mathbf{R}_2\mathbf{\Psi}_1+\mathbf{R}_3\mathbf{\Psi}_2+\mathbf{\Psi}_3 \tag{14}$$

The generalized case yields the vector function $\boldsymbol{\xi}=\left[\xi^{(x)} \quad \xi^{(y)} \quad \xi^{(z)}\right]^T$, such that

$$\boldsymbol{\xi}(\mathbf{q})=\prod_{i=1}^{n+m}\mathbf{R}_i\mathbf{\Gamma}+\sum_{j=1}^{n+m}\left(\prod_{i=j+1}^{n+m-1}[\mathbf{R}_i]\mathbf{\Psi}_j\right)+\mathbf{\Psi}_{n+m} \tag{15}$$

where $\mathbf{q}=\left[\mathbf{u}^T \quad \mathbf{v}^T\right]^T$, $\mathbf{u}=[u_1 \quad \ldots \quad u_n]^T$, and $\mathbf{v}=[v_1 \quad \ldots \quad v_m]^T$. This is a general sweep of a *n*-dimensional geometric entity. Indeed, a similar sweep equation can be defined as

$$\boldsymbol{\xi}(\mathbf{q})=\mathbf{R}(\mathbf{v})\mathbf{\Gamma}(\mathbf{u})+\mathbf{\Psi}(\mathbf{v}) \tag{16}$$

where in this case not only $\mathbf{\Gamma}$ has many parameters but the path could also be an *m*-dimensional entity. The significance and need for this formulation is evidenced in problems arising in robotics, solid modeling, and computer graphics. For example, consider the robot shown in Fig. 6. The kinematic skeleton of the arm is shown in Fig. 6b where joints are characterized by $q_i;\ i=1,\ldots,4$. The vector describing the workspace of a point *P* on the end-effector of the manipulator is given by $\boldsymbol{\xi}(\mathbf{q})$, where this point has been repeatedly swept in space and the volume generated by every point touched by the end-effector is called the swept volume or "workspace" in the field of robotics. In this case, the point P is swept first using the angle q_4, the results of which is swept again using the angle q_3, and subsequently using q_2 and q_1. The same can be done for any number of DOF.

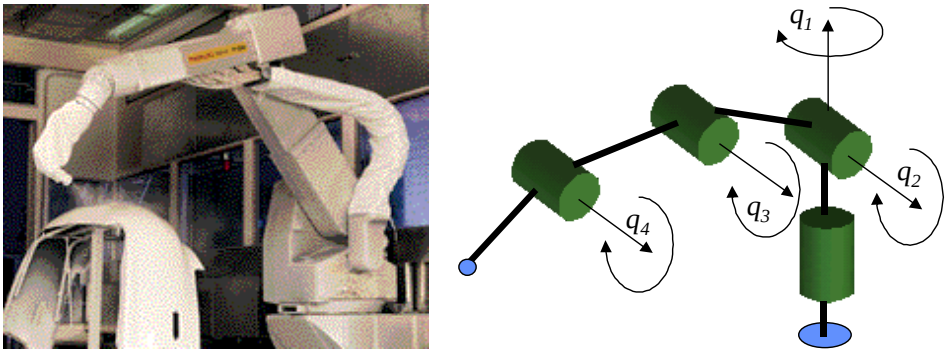

Fig. 6 (a) a robot manipulator (b) the robot's kinematic skeleton

2.4 Deformable Sweeps

Stretching, tapering, and twisting, for example, of an object while it is swept is an important subject and that has become more crucial in recent years for modeling membranes and deformable objects, whether in virtual reality applications or for educations purposes (e.g., modeling of tissues for medical aplications). For example, Sealy and Wyvill (1997) reported a method for generating arbitrary sweep objects, where the object being swept may be a 2D contour or a 3D object. Blackmore *et al*. (1994) extended the SDE approach from rigid sweeps to objects experiencing general smooth deformations. To accomplish this, they observed that an object that is deforming as it is swept along can be modeled by the action of a sweep of the form

$$\xi(\mathbf{x}) = \Psi(\mathbf{v}) + \mathbf{R}(v)\mathbf{x} + \mathbf{N}(\mathbf{x}, t) \tag{17}$$

where $\mathbf{N}(\mathbf{x}, t)$ represents a general nonlinear deformation. Here it is useful to note that when the sweep is rigid, $\mathbf{R}(t)\mathbf{x} + \mathbf{N}$ takes the simple form $\mathbf{R}(t)\mathbf{x}$, where $\mathbf{R}(t)$ is an orthogonal matrix of determinant = 1. Just as in the case of a rigid sweep, the above equation for a deforming sweep leads to a corresponding sweep differential equation (SDE) of the form

$$d\mathbf{x}/dt = d\Psi/dt + (d\mathbf{R}/dt)\mathbf{R}^{-1}(\mathbf{x} - \Psi) - (d\mathbf{R}/dt)P + W \tag{18}$$

where P and W are nonlinear functions associated to the nonlinear portion of the deformation experienced by the swept object.

Once the appropriate SDE (Blackmore and Leu 1990 and Blackmore, et al. 1994) was derived, Blackmore and Leu and their collaborators were able to simply replicate the procedures for rigid sweeps in order to obtain algorithms for the approximate computation of the deforming swept volumes. Very recently Wang *et al*. (2000) extended the sweep-envelope differential equation (SEDE) method, developed by Blackmore and Leu and their associates as an improvement for the SDE, to general deformed swept volumes.

3.0 Formalisms

3.1 Manifold Stratification Method (Jacobian Rank Deficiency)

In differential geometry, a **Manifold with singularities** is defined as a manifold with singular or boundary parts of lower dimensions (e.g., 3, 2, and 1). Because the sweep Jacobian defined by Eq. (11) characterizes the mapping from 3-space to *n*-dimensions it is natural to employ stratification (reduction) of the manifold to many pieces of lower dimensions. A **Stratified space** is defined as a toplogical space which is built up from lower dimensional pieces that are boundaryless manifolds. Based on singularity theory (Spivak 1968, Guillemin and Pollack 1974, and Lu, 1976), Abdel-Malek, et al. (1998) and based on earlier reports (Abdel-Malek and Yeh 1997a; 1997d), were able to show that it is possible to generate the exact boundary envelope of a swept volume using successive stratification of the manifold. Implementation of Jacobian rank deficiency conditions yields a subset of a Euclidean space defined by zeros of a finite number of differentiable functions (called varieties). As a result, **Strata** (plural of the Latin word stratum-layer or level) are defined and used to delineate boundary sub-varieties. Some other aspects of swept volume geometry were also recently analyzed using singularity theory in Blackmore *et al*. (2000).

3.2 Sweep Differential Equation Method and Extensions

An approach to swept volumes that fully exploits the intrinsic geometric and group theoretical structure of Euclidean motions was first presented by Blackmore and Leu (1990) and later developed in detail in Blackmore and Leu (1992a). The key element of this approach is the sweep differential equation (SDE) that is derived from the underlying Lie group structure, which generates the trajectories that determines the geometry of the swept volumes.

More precisely, the boundary of the swept volume of an object can be shown to be subset of the union of (1) the grazing points on the boundary of the object during the entire sweep at which the vector field of the SDE neither points into or out of the object interior, (2) the ingress points at the beginning of the sweep, and (3)

the egress points on the object boundary. A variant of the characterization for grazing curves for the generation of swept volumes was recently developed in Chio and Lee (1999). The grazing points at each time are computed from a tangency function describing the relationship between the sweep vector ant the outward normals for points on the object boundary.

One computationally expensive aspect of the SDE method is that, except for the classes of sweeps defined as autonomous by Blackmore and Leu, the grazing point curves must be computed at every time along the sweep. In order to overcome this computational difficulty, Blackmore *et al*. (1997b) developed an extension of the SDE method that they called the sweep-envelope differential equation (SEDE) approach and presented examples that illustrate successful integration of a prototype SEDE program with commercial NC verification software. The authors reported that the major advantages of an algorithm based on the SEDE method are:

(1) The grazing points set need only be computed at the initial position of the object - the remaining points are generated by the SEDE induced flow of the initial grazing points - so the computational complexity is drastically reduced; and
(2) It provides automatic connectivity for computed boundary points (along trajectories of the SEDE) that facilitates integration with standard algorithms and CAD software for visual realization and Boolean operations.

Algorithms based on the SEDE method have a computational cost that is a full order of magnitude less than those based on the SDE, making them suitable for real-time application in NC machining verification problems and related problems in manufacturing automation. The SEDE algorithm, which was originally developed only for smooth objects, was used together with some novel smooth approximation formulas in order to calculate the swept volume generated by a general 7-parameter APT tool for a large class of sweeps that includes all possible motions in 5-axis NC milling processes in Leu *et al*. (1997). Blackmore *et al*. (1997a) later generalized the SEDE method to piecewise smooth objects and Wang, et al. (2000) have just extended it to deformed swept volumes.

3.3 Parametric, Implicit, and Free Form

Although parametric representations are more widely used and are generally much simpler to treat than implicit representations, swept volumes are widely used in many applications and it is common in solid modeling, for example, to represent solids in implicit forms (simpler to use and to store). In such cases, a CAD program must have the ability to perform sweep operations on the implicitly represented solid without converting the equation to parametric form.

In joint work by the first two authors and associates, a new method for exact determination of sweeps of implicit surfaces was recently presented (Abdel-Malek, et al. 2000a; Abdel-Malek and Yang 2000). The method is briefly summarized here for it provides a new approach to the sweep of implicit surfaces. Consider the sweep equation

$$\xi(\mathbf{w}) = \Psi(t) + \mathbf{R}(t)\Gamma \tag{19}$$

where $\Gamma = [x_1, \ldots, x_M]^T$ and $\mathbf{w} = [\mathbf{x}^T \; t]^T$, and where Ψ and $\mathbf{R}$ are, respectively, smooth (=$\mathbf{C}^\infty$) vector and matrix valued functions with $\Psi(0) = \mathbf{0}$, $\mathbf{R}(0) = \mathbf{I}$ is the identity matrix, and $\mathbf{R}(t)$ is a real (3×3) orthonormal matrix (in the case of the M = 3) for every $t \in [0, 1]$. For the purpose of developing the formulation, it is required only that M be defined as the set of points satisfying finitely many equalities and inequalities for differentiable functions.

In order to develop a method that is consistent and general for any implicit surface, we will represent the surface *M* by a number of inequalities, with no restriction on the number of inequalities nor on the type of variables. Let *M* be represented by

$$M := \left\{ \boldsymbol{\Gamma} :\ \ell_1^L \le f_1(\boldsymbol{\Gamma}) \le \ell_1^U, \ldots,\ \ell_N^L \le f_N(\boldsymbol{\Gamma}) \le \ell_N^U,\ x_1^L \le x_1 \le x_1^U, \ldots,\ x_k^L \le x_k \le x_k^U \right\} \tag{20}$$

where $\mathbf{f} = [f_1, \ldots, f_N]^T$ and $f_i(\boldsymbol{\Gamma})$ denotes an expression representing the surface, ℓ_i is a limit, the upper subscript L indicates the lower limit, U denotes the upper limit, *N* is the number of expressions, and *k* is the number of variables. It should be noted that this is a rather general case, but a surface may be represented by any number of expressions and any number of variables that may or may not have limits.

As a result of this transformation, it is now possible to define the sweep by

$$\boldsymbol{\Phi}(\mathbf{z}) := \begin{bmatrix} \boldsymbol{\xi}(\mathbf{w}) \\ f_1(\mathbf{x}) - 0.5(\ell_1^U + \ell_1^L) - 0.5(\ell_1^U - \ell_1^L)\sin\lambda_1 \\ \cdots \\ f_N(\mathbf{x}) - 0.5(\ell_N^U + \ell_N^L) - 0.5(\ell_N^U - \ell_N^L)\sin\lambda_N \\ x_1 - 0.5(x_1^U + x_1^L) - 0.5(x_1^U - x_1^L)\sin\lambda_{N+1} \\ \cdots \\ x_M - 0.5(x_M^U + x_M^L) - 0.5(x_M^U - x_M^L)\sin\lambda_{N+M} \\ t - 0.5 - 0.5\sin\lambda_{N+M+1} \end{bmatrix} \tag{21}$$

where $\mathbf{z} = \left[x_1, \ldots, x_N, t, \lambda_1, \ldots, \lambda_{N+M+1}\right]^T = \left[z_1, \ldots, z_{2N+M+2}\right]^T$ or using partitioned coordinates $\mathbf{z} = [\mathbf{w}, \boldsymbol{\lambda}_1, \boldsymbol{\lambda}_2]^T$ where $\mathbf{w} = [x_1, \ldots, x_N, t]^T$, $\boldsymbol{\lambda}_1 = [\lambda_1, \ldots, \lambda_N]^T$, and $\boldsymbol{\lambda}_2 = [\lambda_{N+1}, \ldots, \lambda_{N+M+1}]^T$. Note that the parameter *t* has also been included in $\boldsymbol{\Phi}(\mathbf{z})$.

Rank deficiency conditions first developed by Abdel-Malek and Yeh (1997a) can now be applied to determine singular sets of the Jacobian $\boldsymbol{\Phi}_{\mathbf{z}}(\mathbf{z}) = \partial\boldsymbol{\Phi}/\partial\mathbf{z}$ defined by

$$\boldsymbol{\Phi}_{\mathbf{z}} = \begin{bmatrix} \boldsymbol{\xi}_{\mathbf{w}} & \mathbf{0} & \mathbf{0} \\ \mathbf{f}_{\mathbf{w}} & \mathbf{f}_{\boldsymbol{\lambda}_1} & \mathbf{0} \\ \mathbf{I} & \mathbf{0} & \mathbf{w}_{\boldsymbol{\lambda}_2} \end{bmatrix} \tag{22}$$

where $\boldsymbol{\xi}_{\mathbf{w}} = \partial\boldsymbol{\xi}/\partial\mathbf{w}$; $\mathbf{f}_{\mathbf{w}} = \partial\mathbf{f}/\partial\mathbf{w}$; $\mathbf{f}_{\boldsymbol{\lambda}_1} = \partial\mathbf{f}/\partial\boldsymbol{\lambda}_1$; and $\mathbf{w}_{\boldsymbol{\lambda}_2} = \partial\mathbf{w}/\partial\boldsymbol{\lambda}_2$. The Implicit Function Theorem mandates that there not be open sets in the space of $\mathbf{z}$ in which the constraints are redundant. Redundancy occurs when the Jacobian $\boldsymbol{\Phi}_{\mathbf{z}}$, is rank-deficient which will subsequently define *singular surfaces* in the manifold. Singularities as a result of the Jacobian rank deficiency condition are denoted by s_i. The example shown in Fig. 7 was treated using both the SEDE method (Blackmore, *et al.* 1999) and the Jacobian rank deficiency method (Abdel-Malek, *et al.* 2000), where a solid cylinder implicitly defined is swept (with self-intersection).

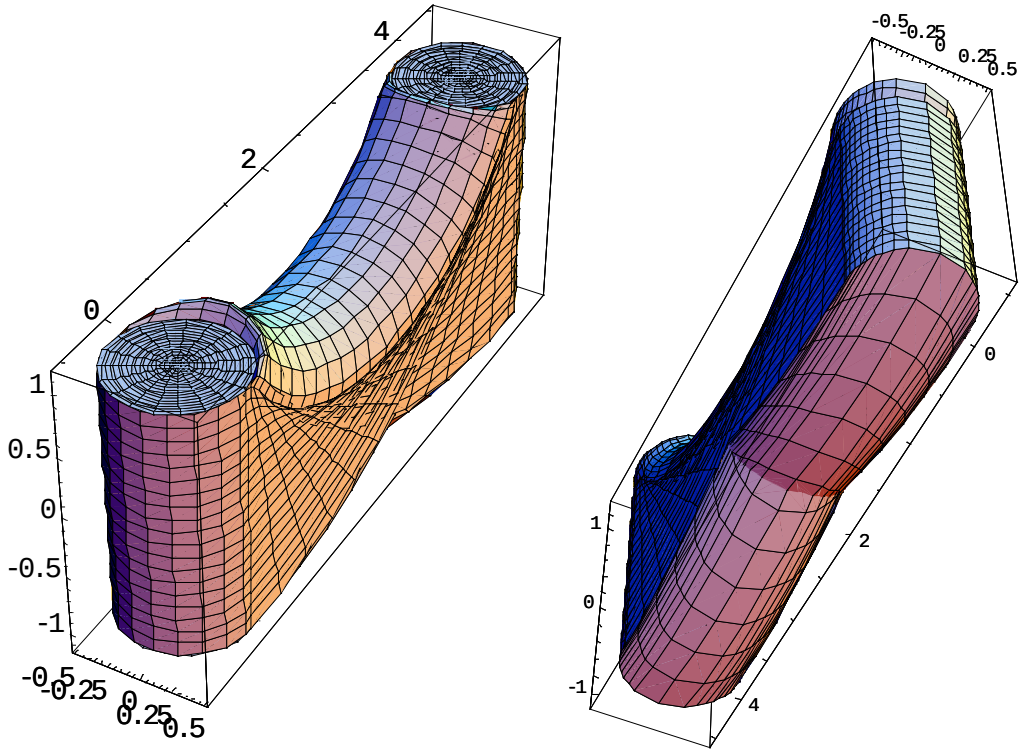

Fig. 7 Two views of the swept volume (same example treated in Blackmore, *et al*. using SEDE trimming methods)

3.4 Identifying the Boundary and Clipping Internal Entities (also called trimming)

To illustrate trimming, consider the simple problem of determining the swept volume of a point on the end-effector of a 2DOF robot manipulator as shown in Fig. 8. Analysis of the equations characterizing the totality of points touched by point *P* yields several curves as shown in Fig. 2b. In order to only depict the boundary (i.e., the envelope) to this workspace, it is necessary to perform clipping (also called trimming) of the internal branches. While this is a simple planar example, this task may prove difficult for complex shapes. Indeed, those curve segments that are to be clipped must first be identified. The result of clipping for this example is shown in Fig. 8c.

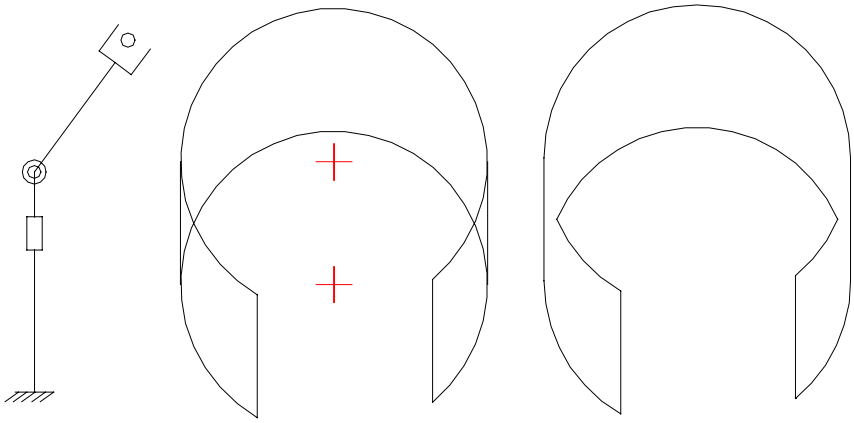

Fig. 8 (a) A 2-DOF robot arm (b) Internal curves as a result of the analysis (c) Trimming curves to delineate the envelope of the swept area (i.e., the workspace of the robot)

A number of methods have appeared that provide solutions to the trimming problem:

(a) Surface-surface intersection. It has been shown that the problem of trimming is best treated using mature surface-surface intersection methods (Bajaj *et al*. 1988, Barnhill and Kersey 1989, Barnhill, et al. 1987, Abdel-Malek and Yeh 1996; 1997b), followed by an elimination procedure such as the perturbation method (Abdel-Malek and Yeh 1997a). Indeed, Blackmore *et al*. (1999) implemented efficient surface-surface methods for both local and global trimming of swept volumes that proved computationally cost effective when combined with approximate calculation and graphical rendering of swept volumes.
(b) Z-buffer (see e.g. Wang and Wang (1986) is a well-known efficient technique used in computer graphics).
(c) Ray-casting (see e.g. Menon and Voelcker 1992 and Menon and Robinson 1993) is a procedure whereby a ray is cast from a point inside the swept volume and intersected with all surfaces. Points of intersection are numbered and their distances computed. Only surfaces with associated points of farthest distance are kept as they must belong to the boundary of the swept volume.

Blackmore *et al*. (1999) developed a particularly efficient algorithm for computing swept volumes that included trimming self-intersections. They first computed a candidate set for the boundary of the swept volume using the SEDE approach and then used the following method to trim the superfluous points: The object was characterized by a piecewise smooth function f that is negative in the interior, positive in the exterior and zero on the boundary of the object. They then defined the function $\varphi_{\mathbf{x}}(t) := f(\eta(\mathbf{x}, t))$, where η represents the reversed flow induced by the SDE. Global trimming was performed for candidate points $\mathbf{x}$ such that $\varphi_{\mathbf{x}}(t)<0$ for some t belonging to the sequence of time steps after local trimming criteria involving first and second time derivatives of $\varphi_{\mathbf{x}}$ had been tested. The computational complexity of their algorithm, including trimming, was shown to be $O(m^2 \log(\log m))$, where m^{-1} is a lower bound for the time steps and the mesh diameter of a triangulation of the boundary of the object.

3.5 Volume and Surface Area Computations

The sweep generation of solid models is a widely accepted technique in dealing with complex shapes occurring in mechanical components such as turbine blades and bevel gears. A key issue in the geometric and mechanical analyses of such elements is the accurate and economical computation of their volumetric properties, namely, their volume, centroid coordinates and inertia tensor. Al-Daccak and Angeles (1989) presented a method for the computation of mass properties for sweep-generated solids based only on their 2D generating contour and their sweeping parameters. The direct 3D calculations of the volumetric properties of swept volumes were reduced to simple 2D calculations. The calculation of geometric or mass properties in CAD systems has been reported in many works (Hoffmann 1989).

Most useful reported techniques for computing the swept volume involve integral identities that convert volume to surface integrals (see a review by Akin 1990). Other methods involve filling the solid with known entities (such as infinitesimal boxes or spheres) to compute the volume. The most widely known technique (Olfe 1995) is computed based on a ray casting procedure whereby the total number of cells of each cross-section is computed using a meshing procedure. The volume is calculated by summing the individual material volumes contained in the cells. An interesting approach to computing the volume of a solid enclosed by a recursive subdivision surface (Peters and Nasri 1997).

4.0 Applications

4.1 Numerically Controlled Machining Verification

Numerically controlled machining verification (known as NC verification) of parts prior to manufacturing leads to higher quality parts and significantly reduced lead times. NC verification is a very cost-effective tool. For NC verification, the method for representing the swept volume removed by a tool as it is manipulated over the workpiece is sometimes called the cutter-swept surface (CSS). Seng and Joshi (1998) proposed a method whereby generated machining volumes are classified using face adjacency relationships of the bounding faces. For example, Sheltami, et al. (1998) proposed a technique that is based on identifying generating curves along the path and connecting them into a solid model of the swept volume.

Parametric representations for the surfaces generated by common NC milling cutters during five-axis motions were extracted using the theory of envelopes by Sambandan and Wang (1989). Also for 5-axis NC verification, surfaces swept by a general tool motion, between the initial and terminal tool positions were represented by several characteristic profiles and parametric definitions of the tool path and orientation vectors (Narvekar, *et al.* 1990 and Narvekar and Oliver 1990).

Some of the works that have addressed NC verification without direct use of swept volume methods include the early work of Voelker and Hunt (1985), Menon and Voelcker (1992), Oliver and Goodman (1990), Takata,et al. (1992), Jerard and Drysdale (1988), Koren and Lin (1995), Menon and Robinson (1993), Oliver and Goodman (1990) and Oliver (1990), Ge (1996), Liang, *et al.* (1997), Liu and Esterling (1997), and Wong and Wong (1998). Liu, et al. (1996) presented an exact geometric model of the volume swept by a tool along a given path. A swept volume-based milling process simulation system was developed for 3-axis milling of complex parts (El Mounayri, et al. 1998). For applications to a toroidal surface, Chung, et al. (1998) presented a procedure for characterizing the cutter-swept surface (CSS) of a generalized tool in a single valued form, $z = f(x, y)$.

A representation of swept volumes based on the topological properties of *n*-dimensional manifolds was presented by Boussac and Crosnier (1996). The algorithm developed for the evaluation of the boundary exploits these properties in such a way that the *n*-dimensional object (swept volume) is generated only from the (*n*-1)-dimensional components resulting from a family of deformations.

More recently, Abdel-Malek, et al. (2000b) modeled the motion of a cutter tool as a surface undergoing a sweep operation along another geometric entity. A topological space describing the swept volume is built as a stratified space with corners. It was shown that varieties appearing inside the manifold representing the removed material are due to a lower degree strata of the Jacobian. Some of the varieties addressed are complicated but can be shown to be reducible because of their parametrization. Figure 9 illustrates material removal. Electric discharge machining has become one of the most accurate machining used for the production of complex manufactured parts.

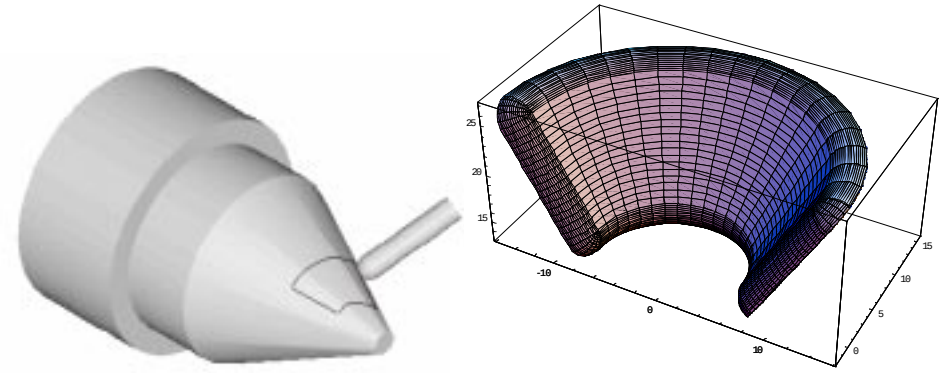

Fig. 9 (a) Tool and workpiece (b) Material removed (swept volume)

The SDE approach was also applied to 5-axis milling in Leu *et al*. (1995). Blackmore *et al*. (1994) later generalized the SDE method to deforming swept volumes and applied this to the analysis of deforming cutting tools in 3-axis NC machining in Leu *et al*. (1998) and the 5-axis machining of sculptured surfaces in Leu *et al*. (1999). In both of these applications the deformed swept volume analysis accounts for cutter deflections and how they affect the resulting objects created by NC machining of simple workpieces.

4.2 Robot Analysis

Swept volumes have been shown to effectively depict the workspace (sometimes called the accessible output set) of serial robot manipulators. These studies are important for understanding robot functionality, dexterity, and their location with respect to targets in a working environment, more importantly their design. Figure 10b, for example, is the workspace of the 4 degree of freedom (4 parameters) shown in Fig. 10a. Only a cross section of the workspace for this 4DOF manipulator was determined by Haug, *et al.* (1996) using a numerical approach (Fig. 10c). It is evident that the swept volume formulation provides a broadly applicable solution to robotic analysis and allows for the determination of the exact boundary and visualization of the volume.

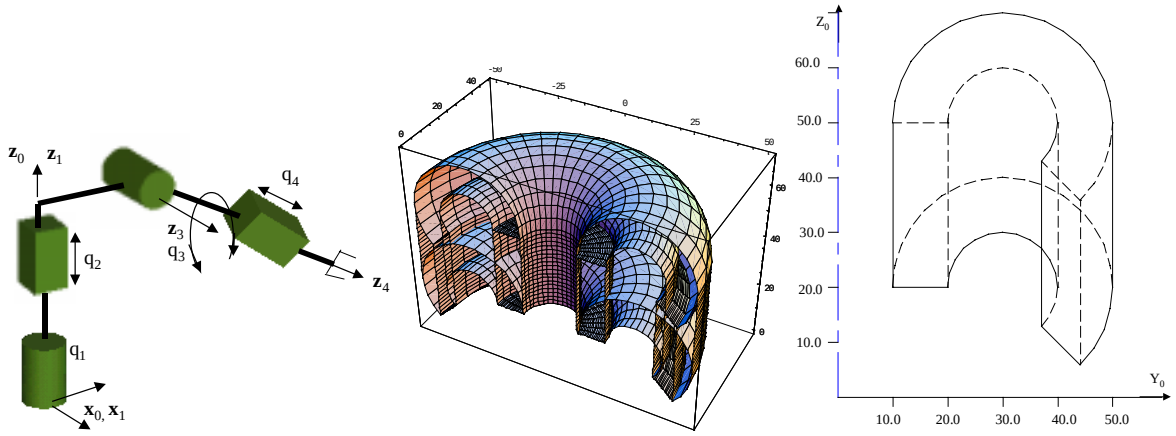

(a) A 4DOF RPRP manipulator (b) The Workspace (c) A cross-sectional plane

Fig. 10 Application of swept volumes to robot analysis

Similarly, real-time motion planning for robots in flexible manufacturing systems (FMS) was addressed by Li and Ma (1996) and Li (1995). Swept volumes were also used in combination with a temporal interval search technique, to compute a series of viewpoints for monitoring a simulated robot operation (Abrams and Allen 1993; 1995). Early works using numerical techniques were presented by Kumar and Waldron (1981) and Kumar (1985) via tracing boundary surfaces of a robot workspace. Tsai and Soni (1981) studied accessible regions of planar manipulators, while Gupta and Roth (1982) and Gupta (1986) studied the effect of hand size on workspace analysis. Other studies on the subject of manipulator workspaces were reported by Sugimoto and Duffy (1982), and Davidson and Hunt (1987), Agrawal (1990), Gosselin and Angeles (1990), Emiris (1993), and Yeh (1996). Zhang, et al. (1996) presented a graphical representation of kinematic workspaces. While all these cited references have addressed the sweep of the manipulator's end-effector, they have been limited to a small number of DOF and are apparently unable to obtain exact surface patches on the boundary. Pennock and Kassner (1993) presented a numerical algorithm for the study of a planar three degree-of-freedom manipulator.

Blackmore *et al*. (1992b; 1992c) also used the SDE approach to classify swept volumes of robot links in two and three dimensions. Equations for general sweeps are derived with the use of homogeneous matrices for representing position and orientation of an object. The corresponding sweep differential equations are obtained from the general sweeps. The tangency condition is used to classify the swept volume of a link element as one of type I or type II.

Numerical criteria were formulated to find the workspace (called the accessible output set) of a general multi-degree-of-freedom system using continuation methods to trace boundary curves suitable for the study of both open- and closed-loop manipulators (Haug *et al.* 1996 and Luh *et al.* 1996). The initial criteria for this computational method were presented by Haug *et al.* (1992) and Wang and Wu (1993). A comparison between the exact method of swept volume computation presented by Abdel-Malek and Yeh (1997a) and the numerical technique used in the above works was jointly presented in a comparative paper by Abdel-Malek, *et al.* (1997).

Singular manifolds (i.e., geometric entities inside the swept volume) in joint space were addressed by Pai and Leu (1992), Burdick (1991; 1992), and Chevallereau and Daya (1994) and Chevallereau (1996). Concepts of crossable and noncrossable surfaces inside a manipulator's workspace were first addressed by Oblak and Kohli (1988).

Exact determination and visualization of the workspace using Jacobian rank deficiency methods was presented by Abdel-Malek, et al. (1997a). Because of the ability to parameterize surface patches on the boundary, it was shown that path trajectory verification could be performed (Abdel-Malek and Yeh 1997c) and placement of the manipulator in its environment to obtain maximum dexterity (Abdel-Malek 1996). The workspace of the manipulator shown in Fig. 11 also has voids (regions inside the workspace that cannot be reached). More recently, control difficulties of the manipulator's end-effector were also addressed (Abdel-Malek and Yeh 2000).

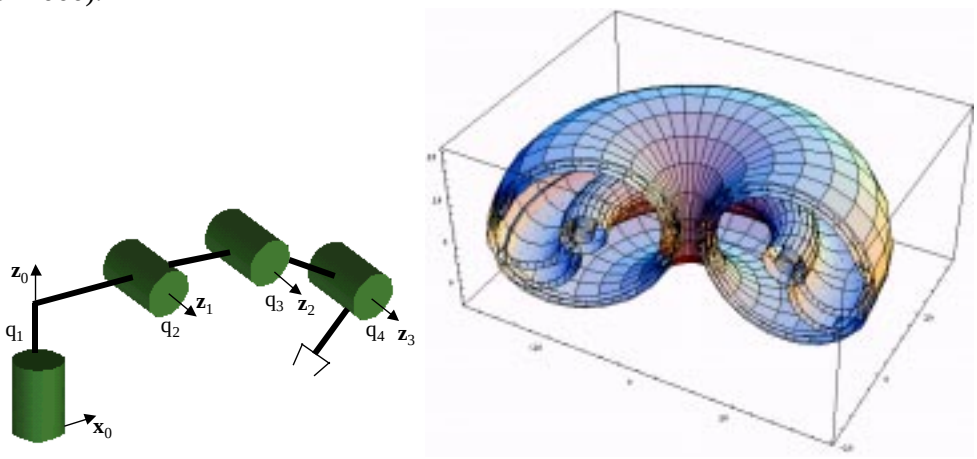

Fig. 11 (a) A four DOF robot (b) Singular surfaces of the workspace (swept volume)

Cecarelli (1995) used an algebraic formulation of a workspace boundary to formulate design equations of three-revolute (3R) jointed manipulators and 4R manipulators (Cecarelli and Vinciquerra 1995) and was also treated by Abdel-Malek, et al. (1999) using the Jacobian rank deficiency method (shown in Fig. 12). All the specified constant angles for this example are $\pi/3$. Only the cross-section was obtained by the first authors using a geometric method for toroidal sweeping.

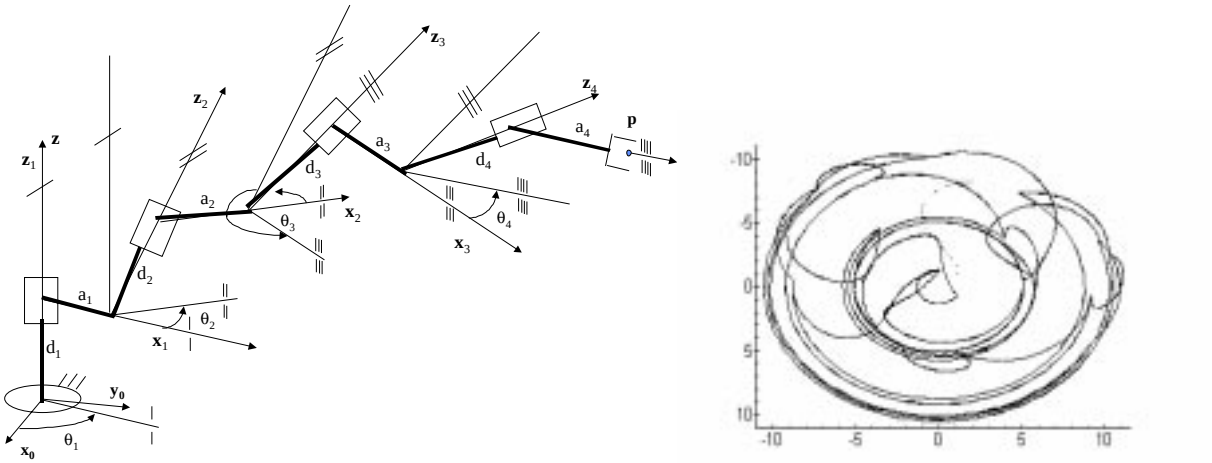

Fig. 12 (a) Workspace of the general 4-DOF manipulator (b) Cross-section at z = 0.8

4.3 Solid Modeling and the Trivariate Freeform Solid

The representation of complex solids using sweep methods has been limited by the difficult mathematics and computational complexity in high-fidelity realistic algorithms. Although some commercial CAD systems offer very limited sweep operations, this type of solid modeling is far from being used on a realistic basis because of the delicate mathematics associated with it. Figure 13 shows a self-intersecting model of a sphere moving along a figure 8 surface depicted using the Jacobian rank deficiency method (Abdel-Malek and Yeh 1997a).

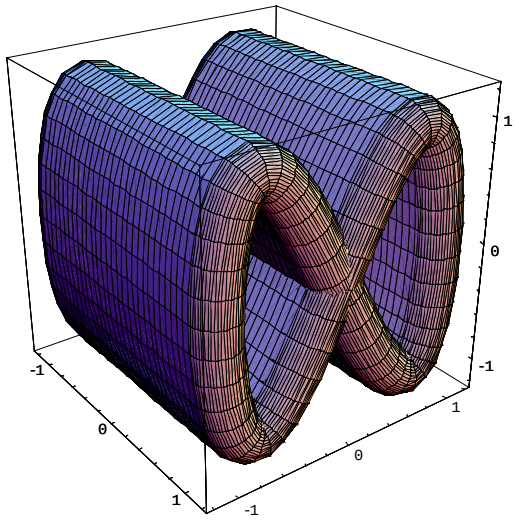

Fig. 13 Solid modeling obtained by sweeping a spherical surface along an 8-shaped surface

The trivariate tensor-product B-spline solid (Casale and Stanton, 1985, Farouki and Hinds, 1985, and Lasser, 1985) is a direct extension of the B-spline patch and has been shown to be useful in the creation and visualization of free-form geometric solids. The trivariate B-spline solid is defined by a set of $(n_1+1)\times(n_2+1)\times(n_3+1)$ control points $\{\mathbf{p}_{i_1,i_2,i_3} : 0 \le i_1 \le n_1, 0 \le i_2 \le n_2, 0 \le i_3 \le n_3\}$, and three sets of knots $\{u_0, u_1, ..., u_{n_1+m_1}\}$, $\{v_0, v_1, ..., v_{n_2+m_2}\}$, and $\{w_0, w_1, ..., w_{n_3+m_3}\}$, where

$$\mathbf{p}(u,v,w) = \sum_{i_1=0}^{n}\sum_{i_2=0}^{n}\sum_{i_3=0}^{n}\mathbf{p}_{i_1,i_2,i_3}N_{i_1,m_1}N_{i_2,m_2}N_{i_3,m_3} \tag{23}$$

or $u \in [u_{m_1-1}, u_{n_1-1}]$, $v \in [v_{m_2-1}, v_{n_2-1}]$, and $w \in [w_{m_3-1}, w_{n_e-1}]$. The products $N_{i_1,m_1} N_{i_2,m_2} N_{i_3,m_3}$ are the trivariate tensor-product B-spline normalized blending functions defined by the knot sequences, and m_1, m_2, m_3 are the orders of the spline in each of the parametric variables. A simple B-spline solid is shown in Fig. 14.

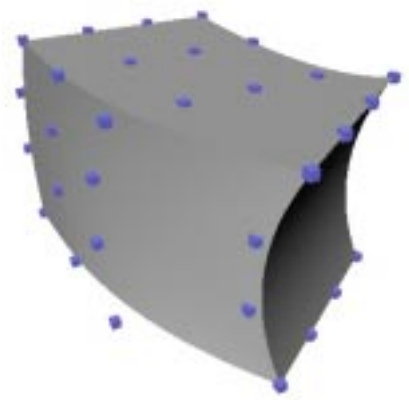

Fig. 14: A cubic trivariate Bézier solid. The solid is defined by 64 control points, shown in blue. The boundary faces are the images of the boundaries of the domain interval.

The trivariate B-spline solid can be considered to be a swept solid, where the generator is a bivariate B-spline patch that continuously changes when being swept along a curve. Here, the B-spline patch is defined by taking any two of the three parameter values of the trivariate solid, and the curve can be defined by the third coordinate.

The B-spline solids have two important features regarding their computation. First, each solid can be refined or subdivided by a trivariate adaptation of the B-spline subdivision algorithm (Boehm, 1980). In the case of the B-spline solid, it can be subdivided in any parameter direction, creating two trivariate B-spline solids whose union is the original one. This property allows the researcher to develop "divide-and-conquer" algorithms to be used for computation on the solids. For example, a B-spline solid may be refined/subdivided into a set of Bézier solids (B-splines with simplified knot sequences) whose union is the original solid (see Farin, 1993). Bounds on the partial derivatives can be obtained using the cone approximations of Sederberg and Parry (1988), Sederberg and Meyers (1988), Kim and Moon (1990), or Kim, et al. (1993).

Visualization of trivariate B-spline solids was first demonstrated by Joy (1991), Reus, et al. (1992), and Joy and Duchaineau (1999). Visualizing these solid objects requires the determination of the boundary surface of the solid, which is a combination of parametric and implicit surfaces. The parametric portion of the boundary is defined as a direct image of the boundary of the domain space, and the implicit portion of the boundary is defined when the Jacobian determinant of the defining function is zero. Joy and Duchaineau (1999) have utilized the Sederberg-Meyers cone approximations to the partial derivatives of the trivariate spline function to establish an interval bound on the Jacobian determinant for a given rectangular cell of the domain space. If zero is not in the interval bound for a given cell, the implicit boundary does not exist in the cell and the trivariate solid can be accurately represented by the images of the bounding faces of the cell. Alternatively, if zero is in the interval bound, the cell is subdivided. Isosurface methods (Lorensen, 1987, Wyvill and McPheeters, 1986, and Shu, 1995) are used to create the surface in a cell where the Jacobian determinant vanishes.

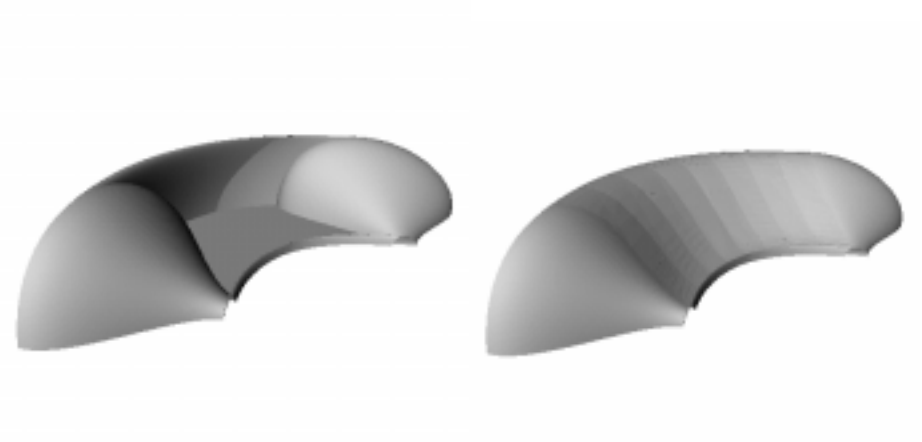

Fig. 15: A trivariate solid approximating a sweep. The picture on the left shows the model with only the boundary face patches, where the picture on the right shows the complete solid.

Joy (1992) and Joy and Madrigal (1999) have utilized two methods to approximate the envelope surface of a swept trivariate B-spline solid. Joy and Madrigal (1999) utilize envelope theory to approximate the swept surface. At a set of points along the path, a characteristic curve was calculated on the envelope, "zippering" these curves to create a polygonal representation of the swept solid. Figure 16 (a) illustrates a complex trivariate B-spline generator, and Figs. 16 (b) and (c) illustrate the results of sweeping this generator along two different paths.

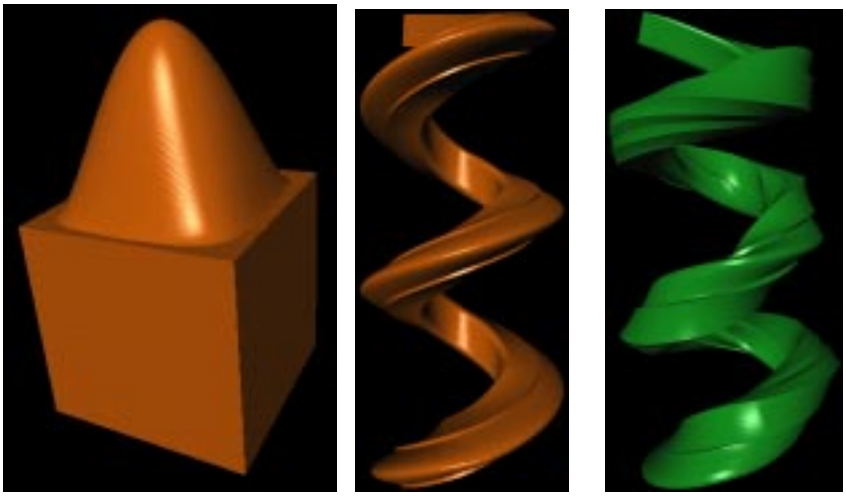

Fig. 16 (a) A trivariate B-spline solid (b) The swept solid defined by sweeping the generator along a spiral curve (c) Sweeping the generator along a spiral curve (with rotations)

4.4 Human Factors (Ergonomics)

Significant attention in recent years has been given to obtaining a better understanding of human joint ranges, measurement, and functionality, especially in conjunction with commands issued by the central nervous system, this research plays a useful role in ergonomic design processes. It has been reported that impaired arms exhibit well-defined workspace deficits as measured by the assisted rehabilitation and measurement (ARM) Guide (Reinkensmeyer, et al. 1999). Researchers have used rigorous kinematic formulations and swept volume technology to model human limbs, understand their workspace, delineate barriers therein where a trajectory becomes difficult to control, and help visualize these barriers. For example, consider modeling the motion of the human arm kinematically as shown in Fig. 17a. The resulting workspace (given

appropriate ranges of motion) is shown in Fig. 17b imposed on the human arm showing the torso (Abdel-Malek, et al. 2000c). The workspace of the index finger, for example, shown in Fig. 18 below is used in the layout design of buttons, levers, and hand tools.

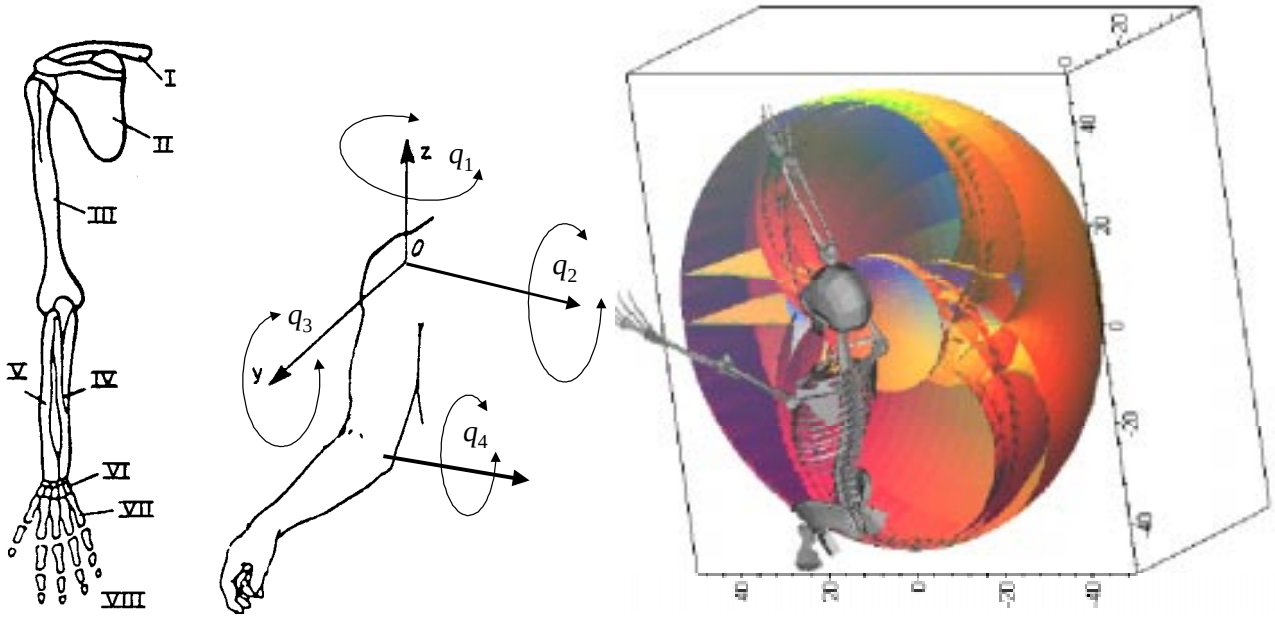

Fig. 17 (a) Joints of the shoulder and elbow are considered (b) Workspace of the hand with respect to the shoulder

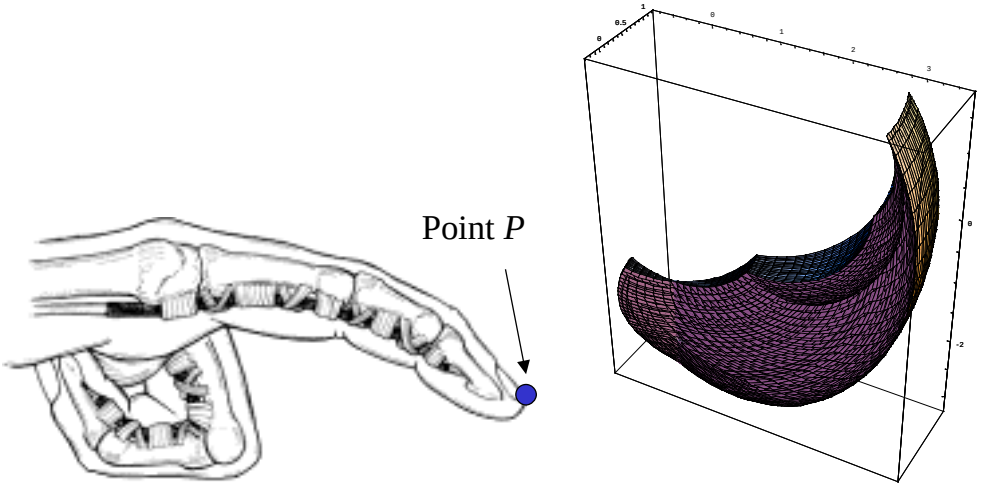

Fig. 18 The workspace of the index finger used in the design of hand tools

Other Applications

In many applications, the motion of objects must be designed such that collision does not occur. Techniques for interference detection that are based on 2-D projections of swept volumes were reported in the early 1990's (Kieffer and Litvin 1990; 1991). Algorithms for the determination of part-removal paths, creation of swept volumes, and representation of large models for interactive visualization were reported by Law, et al. (1998) and were integrated into one system called Galileo. The system is used for maintainability analysis. Xavier (1997) presented an efficient method for computing the exact distance and interference detection for translationally-swept objects. The method was subsequently adapted for rotationally swept objects and reported accurate collision detection. Swept volume technology was also used in Penstroke modeling (Kim, et al. 1993).

Challenges

While the fundamental mathematical foundation for treating swept volumes seems to converge onto rigorous mathematics adapted from Singularity Theory, it is evident that the level of complexity is high. As a result, the main stream of researchers addressing problems pertaining to swept volumes, even in the diverse fields discussed above, has been limited by the difficulty in implementing such algorithms in computer code. Although some commercial mechanical computer aided design codes have limited capability for sweeping, usually in the form of extrude or revolve, it will be some time before a general sweep operation will be available. By general sweep, we mean the ability to repeatedly sweep an object in space to define a complex swept solid. Moreover, while concrete steps have been taken towards the visualization of multivariate solids, substantial effort must be focused on simplifying the mathematical complexity so as to facilitate computer implementation.

5.0 Conclusions

The state-of-the art in the analysis of swept volumes has been presented with emphasis on applications and a review of previous work. Modeling and analysis methods were explored to some extent but were limited to the theoretical foundation rather than the implementation scheme. Challenging applications in diverse fields of manufacturing automation, robotics, solid modeling, and human motion simulation were addressed. It is evident that the topic of swept volumes remains a challenging subject from the standpoint of obtaining faster implementations, better visualization, and more accurate approximations of their boundaries. Nevertheless, there are now solid foundations based upon rigorous mathematics that have and will continue to foster expansion of the breadth of swept volume analysis.

6.0 References

1 Abdel-Malek, K. and Yeh, H.J., 1996 “Determining Intersection Curves Between Surfaces of Two Solids,” *Computer-Aided Design*, Vol. 28, No. 6-7, pp. 539-549.

2 Abdel-Malek, K. and Yeh, H. J., 1997a, "On the Determination of Starting Points for Parametric Surface Intersections," *Computer-Aided Design*, Vol. 29, No. 1, pp.21-35.

3 Abdel-Malek, K. and Yeh, H.J., 1997b, "Geometric Representation of the Swept Volume Using Jacobian Rank Deficiency Conditions”, *Computer Aided Design*, Vol. 29, No. 6, pp. 457-468.

4 Abdel-Malek, K. and Yeh, H.J., 1997c, "Path Trajectory Verification for Robot Manipulators in a Manufacturing Environment" IMechE *Journal of Engineering Manufacture*, Vol. 211, pp. 547-556.

5 Abdel-Malek, K. and Yeh, H.J., 1997d, “Analytical Boundary of the Workspace for General 3-DOF mechanisms,” *International Journal of Robotics Research*. Vol. 16, No. 2, pp. 1-12.

6 Abdel-Malek, K., Adkins, F., Yeh, H.J., and Haug, E.J 1997, "On the Determination of Boundaries to Manipulator Workspaces," *Robotics and Computer-Integrated Manufacturing*, Vol. 13, No. 1, pp.63-72.

7 Abdel-Malek, K., Yeh, H.J., and Othman, S., 1998, " Swept Volumes: Void and Boundary Identification," *Computer Aided Design*, Vol. 30, No. 13, pp. 1009-1018.

8 Abdel-Malek, K., Yeh, H.J., and Khairallah, N., 1999a, "Workspace, Void, and Volume Determination of the General 5DOF Manipulator, *Mechanics of Structures and Machines*, Vol. 27, No. 1, 91-117.

9 Abdel-Malek, K., Seaman, W., and Yeh, H.J., 1999b, “An exact method for NC verification of up to 5-axis machining”, *Proceedings of the 25th ASME Design Automation Conference*, Las Vegas, Nevada.

10 Abdel-Malek, K. and Othman, S. 1999, "Multiple sweeping using the Denavit-Hartenberg Representation Method", *Computer-Aided Design*, Vol. 31, pp. 567-583.

11 Abdel-Malek, K., Yang, J., and Blackmore, D., 2000a, “Closed-form swept volume of implicit surfaces””, *Proceedings of the 26th ASME Design Automation Conference*, Baltimore, MD.

12 Abdel-Malek, K., Seaman, W., and Yeh, H.J., (2000b-in press) “NC Verification of up to 5 Axis Machining Processes Using Manifold Stratification” ASME *Journal of Manufacturing Science and Engineering*.

13 Abdel-Malek, K., Yang, J., Brand, R., Vannier, M., and Tanbour, E. (2000c-submitted), “Towards Understanding the Workspace of Human Limbs”, *International Journal of Ergonomics*.

14 Abdel-Malek, K. and Yang, J., 2000, “Method and Code for the Visualization of Multivariate Solids”, *Proceedings of the 26th ASME Design Automation Conference*, Baltimore, MD.

15 Abrams, S.; Allen, P.K., 1993, “Dynamic sensor planning”, *Proceedings of the IEEE International Conference on Robotics and Automation*, May 2-6, v 2, Atlanta, GA, pp. 605-610.
16 Abrams, S.; Allen, P.K., 1995, “Swept volumes and their use in viewpoint computation in robot work-cells”, *Proceedings of the IEEE International Symposium on Assembly and Task Planning*, Pittsburgh, PA, pp. 188-193.
17 Agrawal, S.K. 1990, “Workspace Boundaries of In-parallel Manipulator Systems,” *Int. J. of Robotics and Automation*, Vol. 7, No. 2, pp. 94-99.
18 Ahn, JC, Kim, MS, Lim, SB, 1997, "Approximate general sweep boundary of 2D curved object", *CVGIP: Computer Vision Graphics and Image Processing*, Vol. 55, pp. 98-128.
19 Akin, J. E., 1990, *Computer-Assisted Mechanical Design*, Prentice Hall, Englewod Cliffs, NJ.
20 Al-Daccak, M.J.; Angeles, J., 1989, “Reduced calculation of volumetric properties of sweep-generated solids”, *ASME (Publication) DE Computer-Aided and Computational Design Advances in Design Automation* - v 19 pt 1, pp. 157-162.
21 Bajaj, C.L., Hoffman, C.M., Lynch, R.E., and Hopcroft, J.E.H., 1988, “Tracing Surface Intersections,” *Computer Aided Geometric Design*, Vol. 5, pp. 285-307.
22 Barnhill, R.E. and Kersey, S.N., 1989, “A Marching Method for Parametric Surface/Surface Intersection,” *Computer Aided Geometric Design*, Vol. 7, pp. 257-280.
23 Barnhill, R.E., Farin, G., Jordan, M., and Piper, B.R., 1987, “Surface/surface Intersection,” *Computer Aided Geometric Design*, Vol. 4, pp. 3-16.
24 Bartels, R., Beatty, J., and Barsky, B., 1987, *An Introduction to Splines for Use in Computer Graphics and Geometric Modeling*, Morgan Kaufmann Publishers.
25 Blackmore, D.; Leu, M. C., 1990, “A differential equation approach to swept volumes”, *Proceedings of Rensselaer’s 2nd International Conference on Computer Integrated Manufacturing*, pp. 143-149.
26 Blackmore, D.; Leu, M.C., 1992a, “Analysis of swept volume via Lie groups and differential equations”, *International Journal of Robotics Research*, v 11 n 6, pp. 516-537.
27 Blackmore, D.; Leu, M.C.; Wang, K.K., 1992b, “Application of flows and envelopes to NC machining”, *CIRP Annals*, v 41 n 1, pp. 493-496.
28 Blackmore, D.; Leu, M.C.; Wang, W., 1992c, “Classification and analysis of robot swept volumes”, *Proceedings of the Japan - USA Symposium on Flexible Automation* Part 1 (of 2), San Francisco, CA, pp. 69-75.
29 Blackmore, D.; Leu, M.C.; Shih, F., 1994, “Analysis and modeling of deformed swept volumes”, *Computer Aided Design*, v 26 n 4, pp. 315-326.
30 Blackmore, D., Leu, M.C., Wang, L.P. and Jiang, H., 1997a, “Swept volumes: a retrospective and prospective view”, *Neural, Parallel & Scientific Computations*, Vol. 5, 81-102.
31 Blackmore, D.; Samulyak, R.; Leu, M.C., 1999, “Trimming swept volumes”, *Computer Aided Design*, v 31 n 3, pp. 215-223.
32 Blackmore, D.; Leu, M.C.; Wang, L.P., 1997b, “Sweep-envelope differential equation algorithm and its application to NC machining verification”, *Computer Aided Design*, v 29 n 9, pp. 629-637.
33 Blackmore, D., Samulyak, R. and Leu, M.C., 2000, “Singularity theory approach to swept volumes”, *Int. J. Shape Modeling*, (in press).
34 Boehm, W., "Inserting New Knots Into B-Spline Curves", *Computer-Aided Design*, Vol. 12, July 1980, 199-201.
35 Boltianskii, V.G., *Envelopes*, Macmillan Publishing, New York, New York, 1964.
36 Boussac, Stephane; Crosnier, A., 1996, “Swept volumes generated from deformable objects application to NC verification”, *Proceedings of the 1996 13th IEEE International Conference on Robotics and Automation*. Part 2 (of 4) v2, Minneapolis, MN, pp. 1813-1818.
37 Burdick, JW, 1991, “A Classification of 3R regional manipulator singularities and geometries” *Proceedings of the IEEE Int. Conference on Robotics and Automation*, Sacramento, CA, pp. 2670-2675.
38 Burdick, JW, 1992, “A recursive method for finding revolute-jointed manipulator singularities”, *Proceedings of the IEEE International Conference on Robotics and Automation*, Nice, France, pp. 448-453.
39 Casale, M.S., and Stanton, E.L., 1985, "An Overview of Analytic Solid Modeling", *IEEE Computer Graphics and Applications*, Vol 5, No. 2, pp. 45-56.
40 Ceccarelli, M. and Vinciguerra, A., 1995, “On the Workspace of General 4R Manipulators,” *International Journal of Robotics Research*, Vol. 14, No. 2, pp. 152-160.
41 Ceccarelli, M., 1995, “A Synthesis Algorithm for Three-Revolute Manipulators by Using an Algebraic Formulation of Workspace Boundary,” *ASME J. of Mechanical Design*, 117(2A), pp. 298-302.
42 Chevallereau, C. and Daya, B., 1994, “A new method for robot control in singular configurations with motion in any Cartesian direction”, *Proceedings of the IEEE International Conference on Robotics and Automation*, Vol. 4, San Diego, CA, pp. 2692-2697.

43 Chevallereau, C., 1996, “Feasible trajectories for a non redundant robot at a singularity” *Proc. of IEEE International Conference on Robotics and Automation*, Minneapolis, MN, pp. 1871-1876.
44 Chou, C.J., and lee, Y.S., 1999, “A shape generating approach for multi-axis machining G-buffer models,” Computer Aided Design, Vol. 31, pp. 761-776.
45 Chung, Y.C.; Park, J.W.; Shin, H.; Choi, B.K., 1998, “Modeling the surface swept by a generalized cutter for NC verification”, *Computer Aided Design*, Vol. 30, No.8, pp. 587-94.
46 Dahlberg, B., and Johansson, B., 1987, "Envelope curves and surfaces", *The Mathematics of Surfaces II*, University Press, 419-426.
47 Denavit, J., and Hartenberg, R.S., 1955, “A Kinematic Notation for Lower-pair Mechanisms Based on Matrices,” *Journal of Applied Mechanics, ASME*, Vol. 22, pp. 215-221.
48 Davidson, JK and Hunt, 1987, “Robot Workspace of a Tool Plane: Part I – a ruled surface and other geometry”, *Journal of Mechanisms, Transmissions, and Automation in Design*, Vol. 109, pp. 50-60.
49 El Mounayri, H.; Spence, A.D.; Elbestawi, M.A., 1998, “Milling process simulation - a generic solid modeller based paradigm”, *Journal of Manufacturing Science and Engineering, Transactions of the ASME*, v 120 n 2, pp. 213-221.
50 Elber, G, 1997, “Global error bounds and amelioration of sweep surfaces,” *Computer Aided Design*, Vol. 29, pp.441-447.
51 Elber, G. and Kim, M.S., 1999, “Offsets, sweeps, and Minkowski sums”, *Computer-aided Design*, Vol. 31 (3), pp. 163**.**
52 Emiris, D.M., 1993, “Workspace Analysis of Realistic Elbow and Dual-elbow Robot,” *Mechanisms and Machine Theory*, Vol. 28, No. 3, pp. 375-396.
53 Farin, G., *Curves and Surfaces for Computer Aided Geometric Design*, Academic Press, 1997.
54 Flaquer, J., Gárate, G., and Parggada, M., "Envelopes of Moving Quadric Surfaces",*Computer Aided Geometric Design*, Vol. 9, No. 4, 299-312.
55 Ganter, M A, Storti, D W, and Ensz, M T, 1993, “On Algebraic Methods for Implicit Swept Solids with Finite Extent’ ASME DE Vol 65(2), pp. 389-396.
56 Ganter, M., Uiker, J., 1986, “Dynamic Collision Detection using Swept Solids,” *ASME Journal of Mechanism, Transmission, and Automation in Design*, Vol. 108, pp. 549-555.
57 Ge, Q.J., 1996, “Kinematics-driven geometric modeling: a framework for simultaneous NC tool-path generation and sculptured surface design”, *Proceedings of the 1996 13th IEEE International Conference on Robotics and Automation*. Part 2(2) Minneapolis, MN, pp. 1819-1824.
58 Gosselin, C. and Angeles, J., 1990, “Singularity Analysis of Closed Loop Kinematic Chains,” *IEEE Trans. on Robotics and Automation*, Vol. 6, No. 3, pp. 281-290.
59 Guillemin, V. and Pollack, A., 1974, *Differential Topology*, Prentice-Hall.
60 Gupta, K.C, 1986, “On the Nature of Robot Workspace,” Int. J. Rob. Res., 5(2) 112-121 (1986)
61 Gupta, K.G. and Roth, B. 1982, “Design Considerations for Manipulator Workspace,” ASME *Journal of Mechanical Design*, Vol. 104, No. 4, pp. 704-711.
62 Hartquist, E.E. Menon, J.P. Suresh, K. Voelcker, H.B. and Zagajac, J., 1999, “A computing strategy for applications involving offsets, sweeps, and Minkowski operations”, *Computer-aided Design*, Vol. 31(3), pp. 175-183.
63 Haug, E.J., Luh, C.M., Adkins, F.A., and Wang, J.Y., 1996, “Numerical algorithms for mapping boundaries of manipulator workspaces,” ASME *J. Mech. Design*, 118, pp. 228-234.
64 Haug, E.J., Wang, J.Y., and Wu, J.K., 1992, “Dextrous Workspaces of Manipulators: I. Analytical Criteria,” *Mech. Struct. and Mach.*, (E.J. Haug, ed.), Vol. 20, No. 3, pp. 321-361.
65 Hoffman, C M, 1989, *Geometric and Solid Modeling, An Introduction*, Morgan Kaufman, Ic., San Mateo, CA, 1989.
66 Hu, Z.; Ling, Z.K., 1995, “Geometric modeling of a moving object with self-intersection”, *Proceedings of the 1995 ASME Design Engineering Technical Conferences*, v 82 n 1, Boston, MA, pp. 141-148.
67 Hu, Z.J.; Ling, Z.K., 1994, “Generating swept volumes with instantaneous screw axes”, *Proceedings of the 1994 ASME Design Technical Conferences*. Part 1 (of 3), v 70 n pt 1, Minneapolis, MN, pp. 7-14.
68 Hu, Z.J.; Ling, Z.K., 1996, “Swept volumes generated by the natural quadric surfaces”, *Computers & Graphics*, v20 n2, pp. 263-274.
69 Jakubowski, R., 1993, “Multiple sweeping in product modeling and analysis”, *Proceedings of the 1993 ASME Winter Annual Meeting*, v 66, New Orleans, LA, pp. 125-133.
70 Jerard, R and Drysdale, R, 1988 ‘Geometric Simulation of Numerical Control Machinery’ *ASME Computers Engineer* Vol 2, pp129-136.

71 Joy, K.I., 1991, "Utilizing parametric hyperpatch methods for modeling and display of free-form solids", *International Journal Computational Geometry and Applications*, Vol. 1, No. 4, 1991, 455-471.
72 Joy, K.I., 1992, "Visualization of Swept Hyperpatch Solids", in *Visual Computing: Integrating Computer Graphics with Computer Vision* (Proceedings of Computer Graphics International '92), T. L. Kunii, ed., Springer-Verlag, Tokyo, pp. 567-582.
73 Joy, K.I. and Duchaineau, M.A., 1999, "Boundary Determination for Trivariate Solids", *Proceedings of the 1999 Pacific Graphics Confernece*, Seoul, Korea.
74 Jüttler, B., and Wagner M.G., 1999, "Rational motion-based surface generation", *Computer-Aided Design*, Vol. 31 (3), pp. 203-213.
75 Kieffer, J.; Litvin, F.L., 1991, "Swept volume determination and interference detection for moving 3-D solids", *Journal of Mechanical Design*, v 113 n 4, pp. 456-463.
76 Kieffer, J.; Litvin, F.L., 1990, "Swept volume determination and interference detection for moving 3-D solids", ASME (Publication) DE, v 24, pp. 309-318.
77 Kim, D.-S., 1990, *Cones on Bézier Curves and Surfaces*, Ph.D. Thesis, Department of Industrial and Operations Engineering, University of Michigan, Ann Arbor, Michigan.
78 Kim, D.-S., Papalambros, P.Y. and Woo, T.C., 1995, "Tangent, Normal, and Visibility Cones for Bézier Surfaces", *Computer Aided Geometric Design*, Vol. 12, pp. 305-320.
79 Kim, M-S, Ahn, J-W, and Lim, S-B, 1993, "An Algebraic Algorithm to Compute the Exact General Sweep Boundary of a 2D Curved Object", *Information Processing Letters*, 47, pp. 221-229.
80 Kim, M.S.; Moon, S.R., 1990, "Rotational sweep volumes of objects bounded by algebraic curves", *Proceedings of the 1990 IEEE International Conference on Robotics and Automation*, pp. 311-316.
81 Klok, F, 1986, "Two Moving Coordinate Frames for Sweeping Along a 3D Trajectory", *Computer-Aided Geometric Design*, Vol 3, pp. 217-229.
82 Koren, Y. and Lin, R.S., 1995, "Five-axis surface interpolators", *Annals of CIRP*, 44(1), 379-382.
83 Kumar, A. and Waldron, K.J., 1981, "The Workspace of a Mechanical Manipulator," *ASME J. Mech. Design*, Vol. 103, pp. 665-672.
84 Kumar, V., 1985, *Robot Manipulators-Workspaces and Geometric Dexterity*, Masters Thesis, The Ohio State University.
85 Lasser, D., 1985, "Bernstein-Bézier Representation of Volumes", *Computer Aided Geometric Design*, Vol. 2, pp. 145-149.
86 Law, C.C.; Avila, Sobierajski;L., Schroeder, W. 1998, "Application of path planning and visualization for industrial-design and maintainability-analysis", *Proceedings of the 1998 Reliability and Maintainability Symposium*, Anaheim, CA, pp. 126-131.
87 Leu, M.C., Blackmore, D. and Maiteh, B., 1999, "Deformed swept volume analysis of NC machining with cutter deflection", *Machining Impossible Shapes*, B.K. Choi and R. Jerard, eds., Kluwer, Boston, 158-166.
88 Leu, M.C.; Blackmore, D.; Wang, L.P.; Pak, K.G., 1995, "Implementation of SDE method to represent cutter swept volumes in 5-axis NC milling", *Proceedings of SPIE - The International Society for Optical Engineering Int. Conference on Intelligent manufacturing*, v 2620 Wuhan, China, pp. 354-364.
89 Leu, M C.; Lu, F; Blackmore, D, 1998, "Simulation of NC machining with cutter deflection by modelling deformed swept volumes", *CIRP Annals - Manufacturing Technology*, v 47 n 1, pp. 441-446.
90 Leu, M C.; Wang, L; Blackmore, D, "Verification program for 5-axis NC machining with general APT tools", *CIRP Annals - Manufacturing Technology*, v 46 n 1 1997, pp. 419-424.
91 Li, W., "Real-time motion planning for robot application in flexible manufacturing systems", *Proceedings of SPIE - The International Society for Optical Engineering Int. Conference on Intelligent Manufacturing*, Jun 10 1995 v 2620, Wuhan, China, pp. 620-625.
92 Li, W.; Ma, C., 1996, "Robot motion planning in flexible manufacturing systems", *High Technology Letters*, v2(2), pp. 1-4.
93 Liang, X, Xiao, T, Han, X, Ruan, JX, 1997, Simulation Software GNCV of NC Verification, Author Affiliation: *ICIPS Proceedings of the 1997 IEEE International Conference on Intelligent Processing Systems*, Part 2 Oct 28-31, Vol. 2, Beijing, China pp. 1852-1856.
94 Ling, ZK and Chase, T 1996, "Generating the swept area of a body undergoing planar motion," *ASME J. Mech. Design*, Vol 118, pp221-233.
95 Liu, C, and Esterling, D, 1997, "Solid Modeling of 4-Axis Wire EDM Cut Geometry", *Computer Aided Design* Vol. 29, No. 12, pp. 803-810
96 Liu, C., Esterling, D.M., Fontdecaba, J., Mosel, E, 1996, "Dimensional verification of NC machining profiles using extended quadtrees", *Computer Aided Design* Vol. 28, No. 11, pp. 845-852.

97 Lorensen, W.E., and Cline, H.E., 1987, "Marching Cubes: {A} High Resolution {3D} Surface Construction Algorithm", *Computer Graphics*, Vol. 21, No. 4, 163-169.
98 Lu, Y.C., 1976, "Singularity Theory and an Introduction to Catastrophe Theory", Springer-Verlag, New York.
99 Luh, C. M. Adkins, F. A. Haug, E. J. and Qiu, C.C., 1996. Working Capability of Stewart Platforms," *ASME J. Mech. Design*, Vol. 118, pp. 220-227.
100 Madrigal, C. and Joy, KI, 1999, "Generating the Envelope of a Swept Trivariate Solid," *Proceedings of the IASTED International Conference on Computer Graphics and Imaging*, Palm Springs, California, October 25-27.
101 Maekawa, T., 1999, "An overview of offset curves and surfaces", *Computer-aided Design*, Vol. 31 (3), pp. 165-173.
102 Martin, R.R.; Stephenson, P.C., 1990, "Sweeping of three-dimensional objects", *Computer Aided Design*, v 22 n 4, pp. 223-234.
103 Martin, R.R.; Stephenson, P.C., 1989, "Swept Volumes in Solid Modellers", *Proceedings of the Third IMA Conference on Mathematics of Surfaces*, Oxford, p. 391.
104 Menon, J.P. and Robinson, D.M. 1993, "Advanced NC verification via massively parallel raycasting, " *ASME manufacturing Review*, Vol. 6, 141-154.
105 Menon, J.P., Voelcker, H.B. 1992, "Toward a comprehensive formulation of NC verification as a mathematical and computational problem", *Proceedings of the 1992 Winter Annual Meeting of ASME*, Vol. 59, Anaheim, CA, pp. 147-164.
106 Narvekar, A.P.; Oliver, J.H., 1990, "Intersection of vectors with general five-axis NC swept volumes", *Proceedings of Manufacturing International '90. Part 4: Advances in Materials and Automation*, Atlanta, GA, pp. 99-104.
107 Narvekar, AP, Huang, Y, and Oliver, J, 1992, "Intersection of rays with parametric envelope surfaces representing five-axis NC milling tool swept volumes", *Proceedings of the 1992 18th Annual ASME Design Automation Conference*, Vol. 44, Scottsdale, AZ, pp. 223-230.
108 Oblak, D. and Kohli, D., 1988, "Boundary surfaces, limit surfaces, crossable and noncrossable surfaces in workspace of mechanical manipulators", *ASME Journal of Mechanisms, Transmissions, and Automation in Design*, Vol. 110, pp. 389-396.
109 Olfe, D. B., 1995, *Computer Graphics for Design, From Algorithms to Autocad*, Prentice Hall, Englewood Cliffs, NJ, 1995.
110 Oliver, J and Goodman, E, 1990, "Direct Dimensional NC Verification" *Computer Aided Design* Vol. 22, pp. 3-9.
111 Oliver, J H, 1990, "Efficient Intersection of Surface Normals with Milling Tool Swept Volumes for Discrete Three-axis NC Verification", *ASME DE* Vol 23(1), pp. 159-164.
112 Pai, D. K. and Leu, M. C. 1992, "Generecity and singularities of robot manipulators. *IEEE Transactions on Robotics and Automation*, Vol. RA-8, pp. 545-559.
113 Parida, L.; Mudur, S.P., 1994, "Computational methods for evaluating swept object boundaries", *Visual Computer*, v 10 n 5, pp. 266-276.
114 Pennock, G.R. and Kassner, D.J., 1993, "The Workspace of a General Planar Three-Degree-of-Freedom Platform-Type Manipulator," *Journal of Mechanical Design*, Vol. 115, pp. 269-276.
115 Peters, J. and Nasri, A., 1997, Computing Volumes of Solids Enclosed by Recursive Subdivision. *Computer Graphics Forum*, Vol. 16(3), pp. 89-94.
116 Reinkensmeyer, DJ, Dewald, JP, and Rymer, WZ, 1999, "Guidance-based quantification of arm impairment following brain injury: a pilot study", *IEEE Trans Rehabil Eng*, 7(1):1-11.
117 Reus, J.F., Mish, K.D. and Joy, K.I., 1992, "Mechanical Deformations of Hyperpatch Solids", *Proceedings of Compugraphics* '92, 147-158.
118 Sambandan, K.; Wang, K.K., 1989, "Five-axis swept volumes for graphic NC simulation and verification", *ASME (Publication) DE Computer-Aided and Computational Design Advances in Design Automation* - v 19 npt 1, Montreal, Que, Can, pp. 143-150.
119 Schroeder, W.J.; Lorensen, W.E.; Linthicum, S., 1994, "Implicit modeling of swept surfaces and volumes", *Proceedings of the 1994 IEEE Visualization Conference*, Washington, DC, pp. 40-45.
120 Sealy, G.; Wyvill, G., 1997, "Representing and rendering sweep objects using volume models", *Proceedings of the 1997 International Conference on Computer Graphics*, Hasselt, Belgium, pp. 22-27.
121 Sederberg, T.W. and Meyers, R., 1988, "Loop detection in surface patch intersections", *Computer Aided Geometric Design*, Vol. 5, No. 2, 161-171.
122 Sederberg, T.W. and Parry, S.R., 1986, "Free-Form Deformation of Solid Geometric Models", *Computer Graphics* (SIGGRAPH '86 Proceedings), Vol. 20, No. 3, pp. 151-160.
123 Seng, Y.-J.; Joshi, S.B., 1998, "Recognition of interacting rotational and prismatic machining features from 3-D mill-turn parts", *International Journal of Production Research*, v 36 n 11, pp. 3147-3165.

124 Sheltami, K.; Bedi, S.; Ismail, F., 1998, “Swept volumes of toroidal cutters using generating curves”, *International Journal of Machine Tools & Manufacture*, v 38 n 7, pp. 855-870.
125 Shu, R., Zhou, C., and Kankanhalli, M.S., 1995, "Adaptive marching cubes", *The Visual Computer*, Vol. 11, No. 4, pp. 202-217.
126 Sourin, A and Pasko, A, 1996, “A function representation for sweeping by a moving solid,” *IEEE Transactions on visualization and Computer Graphics*, Vol 2, pp. 11-18.
127 Spivak, M. 1968, *Calculus on Manifolds*, Benjamin/Cummeings.
128 Sugimoto, K. and Duffy, J., 1982, “Determination of Extreme Distances of a Robot Hand. Part 2: Robot Arms with Sppecial Geometry,” *ASME J. of Mechanical Design*, Vol. 104, pp. 704-712.
129 Takata, S, Tsai, MD, and Inui, M, “1992, “A cutting simulation system for machinability evaluation using a workpiece model,” *Annals of CIRP* 38:539-542.
130 Tsai, Y.C. and Soni, A.H. 1981, “Accessible Region and Synthesis of Robot Arm,” *ASME J. of Mech. Design*, Vol. 103, pp. 803-811.
131 Ueng, W.-D.; Lai, J.-Y.; Doong, J.-L., 1998, “Sweep-surface reconstruction from three-dimensional measured data”, *Computer Aided Design*, v 30 n 10, pp. 791-805.
132 Voelker, H B and Hunt, W A, 1985, ‘The Role of Solid Modeling in Machining Process Modeling and NC Verification’ *SAE Tech. Paper* #810195.
133 Wang, G., Sun, J. and Hua, X., 2000, “The sweep-envelope differential equation algorithm for general deformed swept volumes”, *Computer Aided Geometric Design*, Vol. 17, pp. 399-418.
134 Wang, J.Y. and Wu, J.K. 1993, “Dexterous Workspaces of Manipulators, Part 2: Computational Methods,” *Mechanics of Structures and Machines*, Vol. 21, No. 4, pp. 471-506.
135 Wang, L.; Leu, M.C.; Blackmore, D., 2000, “Generating swept solids for NC verification using the SEDE method”, *Fourth Symposium on Solid Modeling and Applications*, pp. 364-75.
136 Wang, W.P. and Wang, K.K., 1986, “Real-time verification of multi-axis NC programs with raster graphics”, *Proc. IEEE Int. Conf. on Robotics and Automation*, pp. 166-171.
137 Weld, J.D.; Leu, M.C., 1990, “Geometric representation of swept volumes with application to polyhedral objects”, *International Journal of Robotics Research*, Vol. 9 n 5, pp. 105-117.
138 Wellman, B.L., 1957, *Technical Descriptive Geometry*, McGraw-Hill Book Company, New York.
139 Wong, T.N.; Wong, K.W., 1998, “Feature-based design by volumetric machining features”, International Journal of Production Research, v 36 n 10, pp. 2839-2862.
140 Wyvill, B., McPheeters, C., and Wyvill, G., 1986, "Animating Soft Objects", The Visual Computer, Vol. 2, No. 4, 1986, 235-242.
141 Xavier, P.G., 1997, “Fast swept-volume distance for robust collision detection”, Proceedings of the 1997 IEEE International Conference on Robotics and Automation, ICRA. Part 2 (of 4) v 2 Albuquerque, NM, pp. 1162-1169.
142 Yeh, HJ, 1996, Singularity and Workspace Analyses of Serial Robot Manipulators, Ph.D. Dissertation, The University of Iowa, Iowa City, IA.
143 Zhang, S.J., Sanger, D.J., and Howard, D., 1996, “Workspaces of a Walking Machine and their Graphical Representation. Part I: kinematic workspaces,” Robotica, 14, pp. 71-79.
144 Zhou, Y., Chen, B., and Kaufman, A., 1997, "Multiresolution Tetrahedral Framework forRegular Volume Data", Proceedings of IEEE Visualization '97, pp. 135-142.